

# Production of identified charged hadrons vs. Transverse Momentum and Rapidity in p+p collisions at $\sqrt{s} = 62.4$ GeV

I. Arsene,<sup>9</sup> I. G. Bearden,<sup>4</sup> D. Beavis,<sup>1</sup> S. Bekele,<sup>8</sup> C. Besliu,<sup>7</sup> B. Budick,<sup>2</sup>  
H. Bøggild,<sup>4</sup> C. Chasman,<sup>1</sup> H. H. Dalsgaard,<sup>4</sup> R. Debbe,<sup>1</sup> J. J. Gaardhøje,<sup>4</sup>  
K. Hagel,<sup>5</sup> A. Jipa,<sup>7</sup> E. B. Johnson,<sup>8</sup> R. Karabowicz,<sup>3</sup> N. Katrynska,<sup>3</sup> E. J. Kim,<sup>8, \*</sup>  
T. M. Larsen,<sup>4</sup> J. H. Lee,<sup>1</sup> G. Løvhøiden,<sup>9</sup> Z. Majka,<sup>3</sup> M. Murray,<sup>8</sup> J. Natowitz,<sup>5</sup>  
B. S. Nielsen,<sup>4</sup> C. Nygaard,<sup>4</sup> D. Pal,<sup>8</sup> C. Ristea,<sup>4</sup> D. Röhrich,<sup>6</sup> S. J. Sanders,<sup>8</sup>  
P. Staszal,<sup>3</sup> T. S. Tveter,<sup>9</sup> A. Qviller,<sup>9</sup> F. Videbæk,<sup>1</sup> H. Yang,<sup>6</sup> and R. Wada<sup>5</sup>

(The BRAHMS Collaboration)

<sup>1</sup>*Brookhaven National Laboratory, Upton, NY 11973-5000, U.S.*

<sup>2</sup>*New York University, New York 10003*

<sup>3</sup>*Smoluchowski Inst. of Physics, Jagiellonian University, Krakow, Poland*

<sup>4</sup>*Niels Bohr Institute, Blegdamsvej 17, University  
of Copenhagen, Copenhagen 2100, Denmark*

<sup>5</sup>*Texas A&M University, College Station, Texas, 17843*

<sup>6</sup>*University of Bergen, Department of Physics and Technology, Bergen, Norway*

<sup>7</sup>*University of Bucharest, Bucharest, Romania*

<sup>8</sup>*University of Kansas, Lawrence, Kansas 66045*

<sup>9</sup>*University of Oslo, Department of Physics, Oslo, Norway*

(Dated: August 4, 2008)

## Abstract

The BRAHMS experiment at the Relativistic Heavy Ion Collider (RHIC) has measured hadron invariant cross sections for identified charged hadrons for rapidities  $-0.2 < y < 3.8$  in p+p collisions at  $\sqrt{s} = 62.4$  GeV. The data extends the knowledge of production of soft hadrons at lower c.m. energies and serves as a baseline for the heavy ion measurements at RHIC. Transverse momentum spectra are compared to NLO pQCD calculations and to PYTHIA calculations. Pion spectra are well described by at mid-rapidity and quite well at large rapidities by Next To Leading Order pQCD. The net-proton distributions are not well described by default PYTHIA calculation, only when including the advanced popcorn scheme is a reasonable description obtained.

PACS numbers: 25.75.Dw

---

\*Present address: Institute of Proton Accelerator, Chonbuk National University, Jeonju, 561-756, Korea

## I. INTRODUCTION

One of the goals of the relativistic heavy ion program is to study the properties of matter at high temperature and high density. The explorations at the Relativistic Heavy Ion Collider (RHIC) indicate that that at c.m. energies of 200 GeV per nucleon pair indeed such system is formed with novel properties as characterized through the particle production[1–4]. Some of these conclusions relies on comparison to elementary pp collisions, where such nuclear effects should not be present. The RHIC experiments have explored Au+Au and Cu+Cu collisions at 62.4 GeV which is an intermediate energy between those at the SPS (18 GeV) and the bulk of the RHIC heavy ion program at 200 GeV. The 62.4 GeV was chosen to match the highest energy where data were obtained in the ISR experiments. A review how the ISR data relates to the HI measurements and references to those data is given in Ref.[5] Though to minimize the systematic uncertainty for the comparisons to the heavy ion data a brief run with (polarized) pp at 62.4 GeV was carried out to collect pp reference data by the BRAHMS, PHENIX and STAR experiments. There is also considerable current interest in understanding the large transverse single spin asymmetries for pions observed in pp collisions in the energy range from 20 to 200 GeV [6–8] in the framework of different approaches in pQCD [9] Feng, Qui Stermann)]. These measurements are at large values of  $x_F$  so it is of importance for the theoretical studies which relies on higher order QCD effects to understand how well NLO pQCD can describe inclusive spectra of pions and kaons at large value of rapidities. In the paper by Bourrely and Soffer[10] it was argued that pQCD fails badly in the description of  $\pi^0$  spectra at large  $x_F$  at forward angles at 53 GeV[11]. Additional high quality measurements of identified charged hadrons at high rapidity at 62.4 GeV will shed additional light on the validity of pQCD in describing such data.

We report measurements of transverse momentum spectra of identified charged hadrons  $\pi$ , K, protons and anti-protons from p+p collisions at  $\sqrt{s} = 62.4$  GeV where the beam rapidity is 4.2 in several narrow rapidity ranges around  $y = 0$  and 1, and in the interval 2.2-3.8.

The paper is organized as follows. In section II we describe first the BRAHMS detector system in its final physics run with details on 3 sub-systems not previously described in detail. This is followed by a discussion on the Particle Identification (PID) methods, and corrections applied to the data. Section III describes the general results, shape of spectra,

rapidity dependences, particle ratios. Section IV embarks on the discussion, a comparison to ISR data taken about 30 years ago, and comparisons to next to leading order perturbative QCD, to the phenomenological model of PYTHIA, and transport models (URQMD and AMPT) that are often used in analysis of relativistic Heavy Ion data.

## II. ANALYSIS

The data used for this analysis were collected with the BRAHMS detector system towards the end of the 2006 run at RHIC during a two week period dedicated to recording data in pp collisions at  $\sqrt{s} = 62.4$  GeV. As mentioned this particular energy matched energies where RHIC in previous heavy ion runs took data for Au+Au and Cu+Cu collisions and is the highest energy where data were obtained at the ISR. The experiment probed  $0.26\text{pb}^{-1}$  of pp collisions.

### A. Detector System

The BRAHMS detector consists of two movable magnetic spectrometers, the Forward Spectrometer (FS) that can be rotated from  $2.3^\circ$  to  $15^\circ$ , and the Mid-Rapidity Spectrometer (MRS) that can be rotated from  $34^\circ$  to  $2.3^\circ$  degrees relative to the beam line, and several global detectors for measuring multiplicities, luminosity, and determining the interaction vertex, and provides a start time (T0) for time-of-flight measurement.

The MRS is a single-dipole-magnet spectrometer with a solid angle of  $\approx 5\text{msr}$  and a magnetic bending power up to 1.2 Tm. Most of the data presented here were recorded at magnetic field settings of 0.4 and 0.6 Tm. The MRS contains two time projection chambers (TPCs), TPM1 and TPM2 sitting in field free regions in front and behind the dipole (D5). This assembly is followed by a two highly segmented scintillator time-of-flight walls, one (TOFW) at 4.51 m and a second (TFW2) at either 5.58 m ( $90^\circ$  setting) or 6.13 m (other angle settings).

The FS consists of 4 dipole magnets D1, D2, D3 and D4 with a bending power of up to 9.2 Tm. The spectrometer has 5 tracking stations T1 through T5. T1 and T2 are TPCs placed in front of and after the second dipole D2. T3, T4 and T5 are drift chambers with excellent position resolution ( $\approx 80\mu\text{m}$ ) with T3 in front of D3, T4 between D3 and D4, and

T5 after D4 and just in front of the particle identifying detectors H2, a segmented time-of-flight wall and the Ring Imaging Detector (RICH)[12]. The magnetic field of the magnet D1-D4 is scaled. For the present data settings of 1/2 of full field was used at 2° and 3° degrees, and 1/4 and 1/6 at 4° and 6°, respectively. Additional details on the BRAHMS experimental setup can be found in ref. [13] and in Ref. [14] for tracking in the MRS. In the present paper we discuss below three detectors sub systems not described in the reference just given, namely the vertex and luminosity detectors, the extended time-of-flight wall in the mid-rapidity, and the spectrometer trigger counters used in the BRAHMS experiment for run-4 through run-6.

Data were taken at spectrometer settings of 90°, 45°, 6°, 4°, 3° and 2.3°. A major goal of the experiment was to measure transverse single spin asymmetries, which have been reported elsewhere [8], with the largest amount of the beamtime spend at the 3° and 2.3° settings.

### *1. Vertex and Luminosity detectors*

A set of symmetrically placed Cherenkov Counters (CC) symmetrically placed at 1.9 (inner ring) and 6.4 meters (outer ring) around the nominal interaction points is used for normalization of the cross section giving the luminosity, providing the vertex and start time for Time-of-flight measurements. Each detector consists of a thick piece of lucite (4.87 cm) backed by a small number of PMTs (8 and 5 in inner rings, 10 in the outer rings). The geometry is such that for most particle hitting the surface of the Lucite direct Cherenkov photoelectrons will arrive at the PMT surface for relativistic particle, though not all. The response from the detector is thus quite complicated, and the detector is not designed for hit counting, but to get a good timing signal and have high efficiency. The inner detector rings have a inner radius of 5.4 cm and an outer of 15 cm, the outer detectors have an inner radius of 6.7 cm and an outer radius of 17.40 cm. The detectors covers the pseudo-rapidity range from  $3.26 < \eta < 5.15$ . The left inner and outer rings, and the outer right ring covers full azimuth while the inner right ring has a cutout for  $120^\circ < \phi < 240^\circ$ . This later cutout is implemented not to interfere with the forward spectrometer. An average timing signals is derived for all tubes hit in the left and right array. The sum and the difference of these represents the start time of the event and the vertex position of the interaction. By comparisons to tracks in the mid-rapidity spectrometer we deduce that the

position resolution is 1.2 cm which corresponds to a time resolution of about 100 psec. Even though the detector covers a large fraction of the available rapidity range, only a small fraction  $\approx 33\%$  of the total inelastic events and 45% of the NSD events give rise to a coincident signal in these detectors at 62.4 GeV. Further details on the detector design and performance will be forthcoming in a technical paper[15].

## 2. *TFW2*

This time-of-flight array consist on 41 slats. The slats are 40 cm high, 5 cm wide and 1.5 cm thick made of BC408 scintillator material. Each end of the slat has a H2431 (2 inch Hamamatsu R2083 assembly) attached with optical cement. The tubes are connected often in pairs to a LeCroy 4032 high voltage mainframe. The anode signal is passively split in the base and one signal goes to an FASTBUS ADC and the other to a disc. for timing. The signal to the disc. either has a low frequency filter box mounted at the tube base. The detectors are built to be symmetric about the axis of the MRS. The detectors are mounted on two arcs. The front arc has a radius of curvature of 508 cm. The center of the arc is the D5 center when the array is at 700 cm. The back arc has a radius of curvature of 512 cm again with the center being the magnet center when the array is at 700 cm. The array is movable and have a distance of 558 cm from the pivot to the front of middle of the array. At the extended position the array is was extended is at 614 cm. The time resolution of the detector is 120 psec.

## 3. *Triggers*

The trigger in the MRS is formed by requiring coincidences between the time-of-flight (TOFW) wall placed at 4.33 m from the nominal interaction point (IP), a hodoscope (TRMRS) placed immediately behind the magnet D5, and the RHIC 9.7 MHz clock. The TRMRS is a 12 slat hodoscope, each slat with a size of 2\*9\*0.4 cm readout by fast phototubes (XXXX) at each end of the slat. The slats were made thin to minimize the multiple scattering for low momentum particles. The TOFW also has readout at each end of the slats as described in ref. [13]. A signal from each phototube was fed into a discriminator converted into into ECL signals and fed into a custom designed programable VME module

which required coincidence overlap between the input from the top and bottom signal from each tube and provided a logic OR. The overlap coincidence time is 20 nsec. Each VME module can handle signals from up to 16 slats, and a set of such modules are daisy-chained to form the logic requirement of one good hit the the respective hodoscope within the resolving time of the unit which is smaller than the bunch crossing time of 107 nsec. In the FS the trigger is formed from a hodoscope (TRFS) placed immediately behind the magnet D1 and in front of T1, the two time-of-flight walls H1 and H2, placed at 8.8m and 18.8 m, respectively, and the RHIC 9.7 MHz clock. The TRFS is a 7 slat hodoscope with dimensions of each slat being 3\*9\*0.4 cm (W\*H\*D) readout by fast phototubes (XXXX) at each end of the slat similar in design to the TRMRS. The triggers in both spectrometer arms thus does not require the minimum bias trigger (CC), and are thus sensitive to events with tracks from the total inelastic pp cross section. Both triggers have been estimated using minimum bias triggers to be more than 99% effective.

## B. Tracking

Local tracks are first determined in the TPCs and DriftChambers which are all situated in field free region. The resulting straight-line track segments in two tracking chambers located on either side of a magnet are matched using the effective edge approximations generating matched tracks.

For the matching using the D4 magnet where the field is has a spatial non uniformity, a second correction to the deduced momentum is applied based on the orbit of the track. The correction was deduced from full geant simulations of the spectrometer using the measured field (or rather TOSCA derived) map for the D4 magnet. Local tracks and local matched tracks are combined in the FS to form complete tracks. The complete track are refitted to deduce the final momentum. Tracks in the FS are required to project through the magnet D1 onto the nominal beamline. Track quality cuts are applied for the final track selection.

Tracking and matching efficiencies for each of the 5 tracking stations in the spectrometer were calculated by constructing full tracks with 4 track segments and evaluating the efficiency in the 5<sup>th</sup> station by comparison to found local segments. The overall tracking efficiency is about 80-90%, and is included in the extraction of the cross sections.

### C. Particle identification

In MRS the particle identification is done using the time-of-flight with the CC time as start and the TFW2 (or TOFW) time as the stop. The TOFW time-of-flight was used for checking result from TFW2. Due to the longer flight path the result from TFW2 results in a larger  $p_T$ -range with good particle ID despite the small reduction in yield due to additional decay and absorption of particles.

To identify charged pions, kaons and protons using the time-of-flight detectors  $3\sigma$  standard deviations cut in  $1/\beta - 1/\beta_C$  where  $\beta_C = |p|/\sqrt{p^2 + m^2}$  is the calculated velocity and  $\beta$  the measured velocity. A typical PID spectrum for  $45^\circ$  is shown in Fig. 1 demonstrating the overall good PID in the MRS. It is noted that in order to make the PID with time-of-flight a vertex and time signal from the CC counters are needed. This has important consequences for the normalization. The resolution in  $1/\beta$  for TFW2 have average values of 0.0055 at

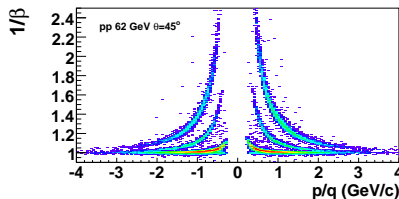


FIG. 1:  $1/\beta$  vs.  $p/q$  with MRS at  $45^\circ$ . (colors online)

$45^\circ$  and 0.007 at  $90^\circ$ . With these resolutions kaons are well separated from pions up to 1.8 GeV/c, while protons are separated from kaons up to 3 GeV/c. The pion spectra can be extended to somewhat higher momenta since the  $K/\pi$  ratio is well below 1 ( $\approx 0.2 - 0.35$ ). An analysis which made slices in the  $1/\beta - 1/\beta_C$  distributions for momenta above 1.8 GeV/c was used to extract the ratio of  $K/\pi$  vs. momentum at  $90^\circ$  and  $45^\circ$ , and to estimate the contamination from kaons in the pion spectrum with a  $3\sigma$  cut. Below 1.9 GeV/c the contamination is negligible, but grows to  $\approx 30\%$  for  $\pi^+$  at 2.6 GeV/c and to 25% for  $\pi^-$  at 2.7 GeV/c. Spectra of pions are presented from the  $90^\circ$  setting up to  $p_T = 2.8$  GeV/c and at  $45^\circ$  setting up to  $p_T = 2.2$  GeV/c.

In the forward spectrometer the particle identification is made primarily with the RICH detector. For all angle and field settings the pions are above threshold and are identified requiring that the measured ring radius is within  $3\sigma$  of the calculated radius on a track-by-

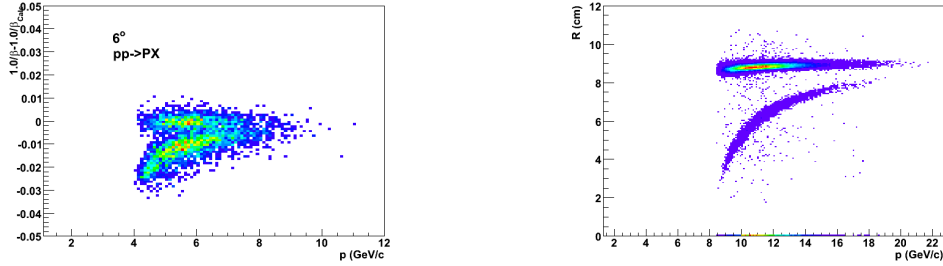


FIG. 2: Left hand side: Particle identification at  $6^\circ$ . Right hand: PID using RICH at  $3^\circ$  and half field.

track basis. The yields are corrected by the efficiency which decreases near the threshold due to fewer Cherenkov electrons emitted. The efficiency is estimated from both measurements using the time-of-flight in H2 and from simulations as described in Ref.[12]. Kaons are identified in the momentum range  $10 < p < 20$  GeV/c using the same technique, with the additional requirement that the measured radius is more than  $3\sigma$  away from the pion radius at a given momentum. The efficiency of the RICH detector has been studied with pions identified with a scintillator time-of-flight counter in an overlapping momentum range and reaches an upper value of 97%. Protons and anti-protons are identified using the RICH in veto mode in the momentum range  $10 < p < 18$  GeV/c. Protons will not produce a signal in the RICH; most pions and kaons will not either in this momentum range, but a small fraction  $\approx 2.8\%$  leaves no signal. The contribution from these events are subtracted on a statistical basis from the protons candidates assuming they constitute 2.8% of the measured pions and kaons in the same setting. For protons this correction is very small, but for anti-protons it results in a roughly 50% systematic uncertainty on the yields. In the momentum range  $5 < p < 8$  GeV/c i.e. for the  $4^\circ$  and  $6^\circ$  settings protons are identified using the time-of-flight in H2 and requiring that no signal is observed in the RICH. This is fairly clean, the purity of the proton sample can be estimated, and the kaon contribution per momentum bin is subtracted in the final analysis. The quality of the PID separation of protons from kaons and pions is illustrated in Fig.2 For anti-protons though the background subtraction is large and results in the estimated systematic uncertainty of 50% on the differential yields at large rapidity.

## D. Corrections

The data are corrected for the spectrometer geometrical acceptance, multiple scattering, weak decays and absorption in the material along the path of the detected particles. To correct for these it is assumed that the geometric acceptance and the correction due to the different physical processes that particles are subject to, can be factorized. This has been confirmed by full Monte Carlo simulation with simulated spectra having similar shapes as the observed spectra that this procedure reproduces the input to better than 4% except for the protons with momenta less than 0.6 GeV/c. An additional correction based on the Monte Carlo calculation is applied here.

The BRAHMS spectrometers are small solid-angle devices. The largest correction to the recorded yield is from geometrical acceptance of the spectrometers. It is evaluated by a purely geometric monte carlo procedure, that is equivalent to what we use for the more sophisticated analysis based on detailed Monte Carlo simulations. Particles are thrown from different positions along the beam line where interactions take place, sorted into vertex bins of 5cm, and we record the probability that the particles traverse the spectrometers at any given field setting, and are hitting the fiducial volumes in question i.e the TFW2 wall, the RICH detector, or the H2 hodoscope. For each particle kind we keep a record of this probability as function of  $y$  and  $p_T$ . The accuracy of this correction is about 1.5%, so even though it is large in order 200, it is very well determined.

The correction due to the interaction particles experience in the spectrometers are evaluated as follows. For each kind of particle  $\pi$ , kaons, protons and anti-protons the correction is evaluated as function of momentum and spectrometer angle setting using the BRAG program, that is based on the GEANT3 libraries[16], describing the BRAHMS detector system. Single particles are tracked by BRAG, the hits in the detectors are digitized and subjected to the same analysis package as real data. The GEANT3 default parameters and cuts are used, except for the hadronic interactions which are evaluated using the FLUKA [REF?] interface. It has been shown to describe particular absorption data for p-bars much better than the GHESIA package. The accuracy of these corrections is estimated to be  $\approx 1\%$  (absolute) on corrections typically 85 – 95%, on top of the trivial decay correction for pions and kaons.

The invariant cross section are calculated from the measured number of counts in a  $y$ - $p_T$  bin,  $N(y, p_T)$  as

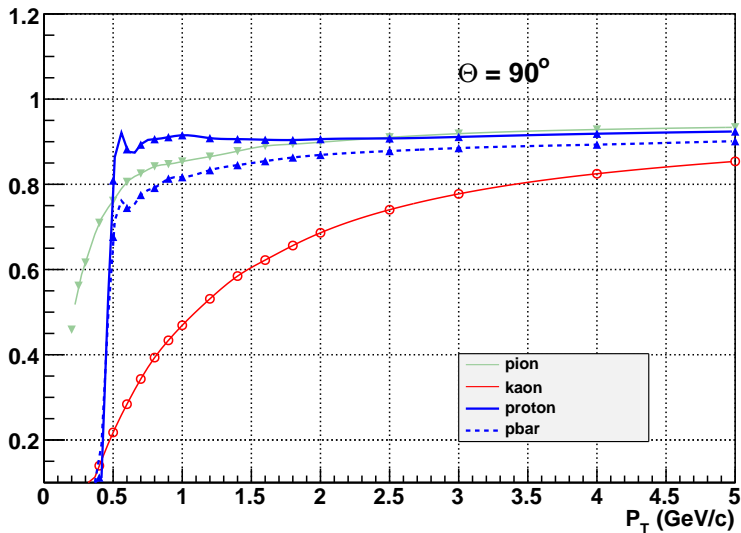


FIG. 3: Efficiency of singles particles of pion, kaons and protons in the MRS.

$$\sigma_{y,p_T} = \mathcal{L}^{-1} N(y, p_t) / (2\pi p_T Acc Eff) \quad (1)$$

The luminosity is deduced from the measured counts with the CC counters from  $N_{cc} = \mathcal{L}\sigma_{CC}$ . The  $\sigma_{CC}$  was evaluated from two separate vernier scans (citation to some CA-note) to be  $12 \pm 1.4$  mb. Since the vertex distribution of pp collisions is rather wide ( $\sigma_Z \approx 50$ cm and the spectrometer acceptance depends on the vertex position, most strongly for the MRS, the specific sums are done with

$$\sigma_{y,p_T} = \mathcal{L}^{-1} \sum_v N(y, p_t, v) / \sum_v 2\pi p_T Acc(v) Eff \quad (2)$$

This particular summing preserves the proper Poisson statistics in case of bins within acceptance and with 0 counts.

As mentioned earlier the CC counters are only sensitive to about 40% of the NSD cross section. Therefore, there is a bias towards selecting events with a high multiplicity of particles when the global vertex is required for event selection. This correction is needed when the PID is done with time-of-flight both in the MRS and in the FS, but not when identifying particles based on the information in the RICH detector, or when no particle identification is done. This bias can also have a  $p_T$ -dependence. This  $p_T$ -dependence was evaluated from the data using RICH information only comparing  $p_T$  spectra with and without the requirement

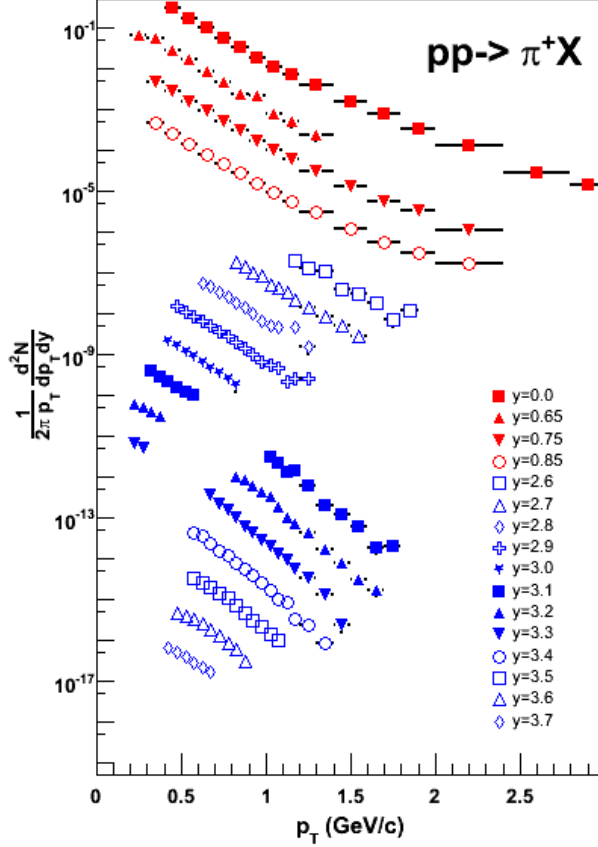


FIG. 4: Invariant transverse  $p_T$  spectra for  $\pi^+$  for rapidities as indicated in the figure. Each rapidity bin is scaled down by a factor of 10 from the previous.

of a global vertex. In the MRS the effect is quit small for  $p_T < 3.0$  GeV/c, and in the FS for  $p_T < 1$  GeV/c.

The spectra presented here has not been corrected for feeddown from the weak decays of  $K_s^0, \Lambda$  etc. It has been studied in details for Au+Au reactions at 200 GeV. (ref EJK, DO) In those reactions the  $K/\pi$  and  $\Lambda/p$  ratios are higher, 0.2 and 0.9 respectively, than expected for the p+p reactions presented here [reference to Lambda ratios]. The expected ratio  $\Lambda/p$  is  $\approx 0.4$  at 62 GeV. We can thus estimated the contribution to the pion spectra from weak decays to be less than 2%. At the lower  $p_T$  the BRAHMS spectrometers accepts and identifies most of the protons from  $\Lambda$  decays, albeit at somewhat higher pt this is not the case. We refer the reader to [14] for additional details.

[summary needs ref to pp- energy syst ; should we give the corrections?]

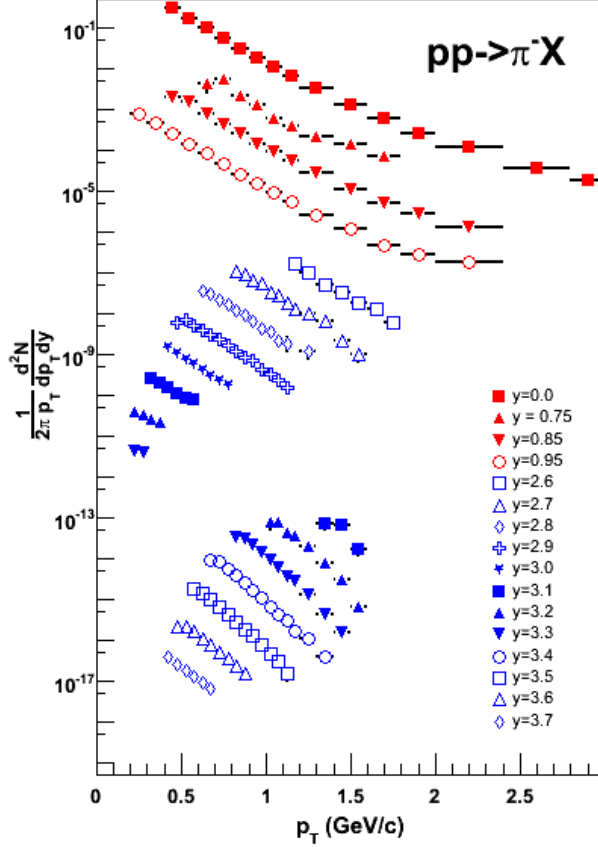


FIG. 5: Invariant transverse  $p_T$  spectra for  $\pi^-$  for rapidities as indicated in the figure. Each rapidity bin is scaled down by a factor of 10 from the previous.

### 1. Systematic uncertainties

The spectrum data have been corrected for several effect, some of which have been discussed in the previous sections. In the section we summarize the effects, typical values and estimates of the systematic uncertainty associated with each.

- Yield corrections from tracking, efficiencies in tracking detectors, matching efficiencies matches of spectrometer tracks to the beamline and/or vertex determined by the CC counters.
- geometric acceptance.
- PID corrections. Intrinsic efficiency of the RICH or Time-of-flight detectors, efficiency of matching of tracks to hits.

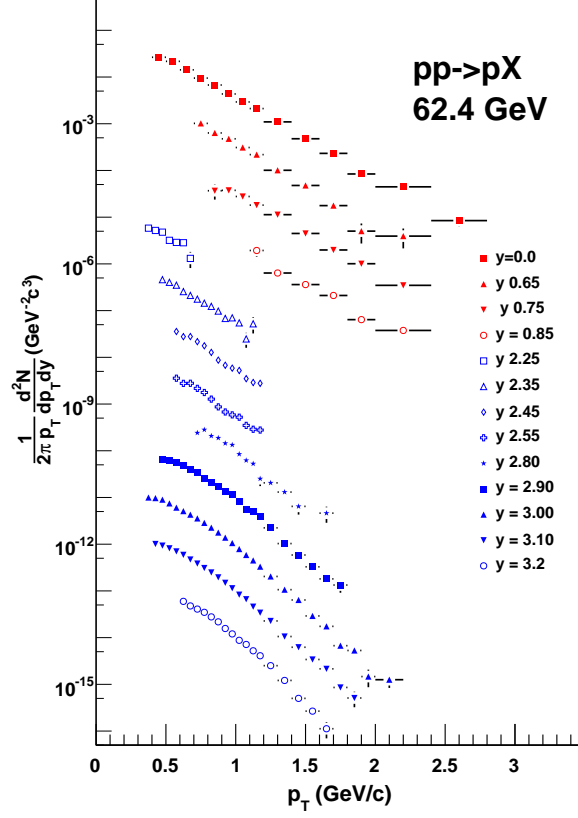


FIG. 6: Invariant transverse  $p_T$  spectra for protons for rapidities as indicated in the figure. Each rapidity bin is scaled down by a factor of 10 from the previous.

- Corrections for losses due to absorption (Nuclear interactions), multiple scattering, weak decays of  $\pi$  and  $K$
- Uncertainties in determinations of events normalization, including effect of Vernier scans.

	typical value	syst uncertainty	From
tracking efficiency	0.65-0.80	4	determined from data
PID-RICH	0.97	1	data and simulations
Normalization	0.82	10	Vernier scan

The systematic uncertainties on the  $p_T$  spectra shown in this chapter arise from the cuts and corrections which are applied to the data. The charged hadron spectra are subject to the following cuts which determine the systematic uncertainties

- matching of local tracks between the TPCs

- comparing track vertices to the primary vertex (where the Z-direction is obtained from the BBCs or the CCs),
- tracking efficiency
- matching tracks with hits in the PID detector and selection values
- PID efficiency
- correction for multiple scattering, absorption and decay
- trigger inefficiency for the p + p collisions
- spectrum construction method

### III. RESULTS

The invariant spectra for  $\pi^+$ ,  $\pi^-$  are shown in Fig.6,7. The invariant cross sections are normalized to the total inelastic cross section of 36 mb. The spectra for each rapidity bin, as indicated in the figure, are scaled by a factor of 10.

general properties of spectra.

Particle ratio's mid-rapidity , forward rapidities.

fit fct if possible

dn/dy under certain assumptions on spectral shape?

dn/dy for pt

should be given as cross sections (available as dn/dy in tables?)

pions -y=0, 1, 2.6-3.2

protons same

kaons 0,1,3.0

charged hadrons (+,-) treated as pions.

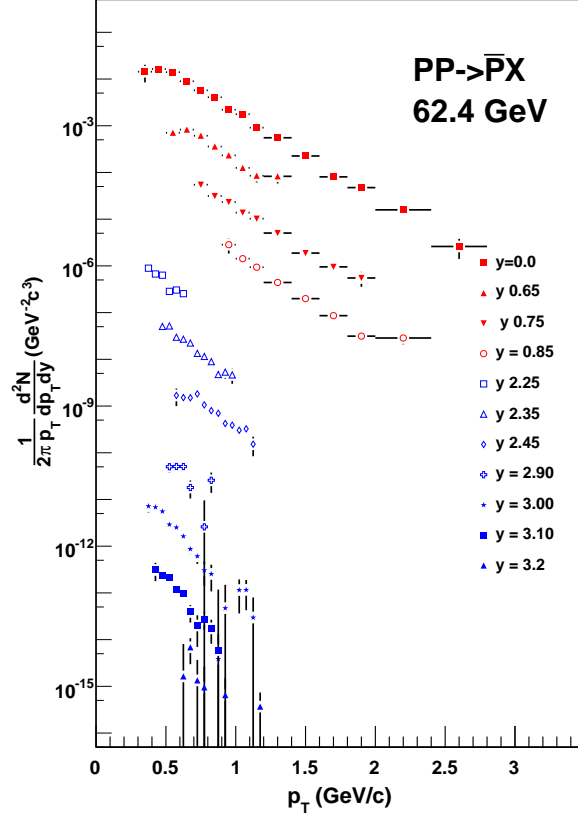


FIG. 7: Invariant rapidity densities for anti-protons for rapidities as indicated in the figure. Each rapidity bin is scaled down by a factor of 10 from the previous.

#### IV. DISCUSSION

There is considerable interest in understanding the energy and rapidity region where perturbative QCD is applicable. This is in regard to understand particle production at mid-rapidity in pp as a reference for the heavy ion experiments, and as a baseline for understanding transverse spin asymmetries at large values of  $x_F$ . The data for  $\pi^+$  and  $\pi^-$  production at two forward rapidity values where the reach in  $p_T$  is largest, namely 2.7 and 3.1 are compared to Next to Leading Order pQCD calculations. The conditions used in the calculations are described in detail in [17]. In short the calculations are evaluated at equal factorization and renormalization scale  $\mu = \mu_F = \mu_R = p_T$  using the CTEQ6 parton distribution functions and the modified “Kniehl-Kramer-Potter” (KPP) fragmentation functions. The comparison is shown in Fig.13 for  $\pi^-$  at  $y=2.7$  and 3.1 and for  $\pi^+$  in Fig.???. The agreement is in fairly good agreement on the absolute magnitude, and in describing the change from 2.7 to 3.1 in

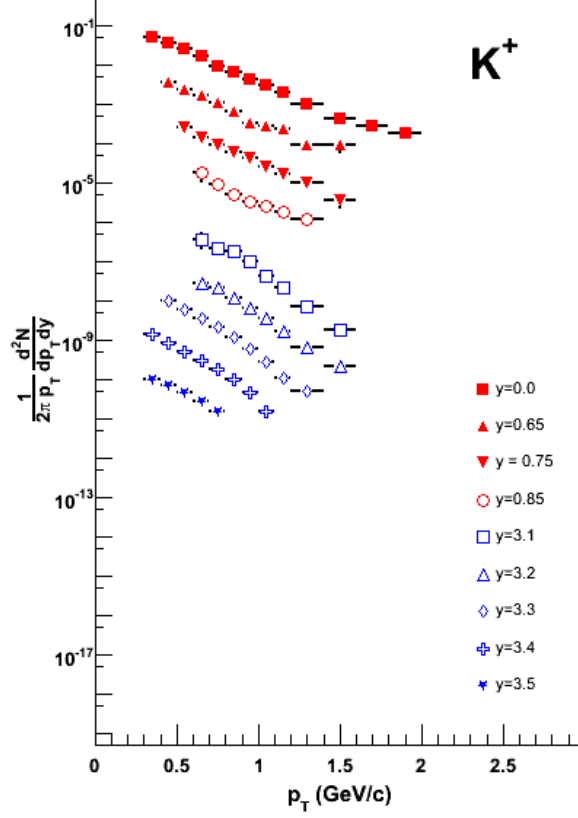


FIG. 8: Invariant rapidity densities for  $K^+$  for rapidities as indicated in the figure Each rapidity bin is scaled down by a factor of 10 from the previous (prelim Data for FSLF not corrected for purity)

rapidity. There is though a trend towards underestimating the data at the highest  $p_T$  values. At first glance this is in disagreement with the conclusions of Ref.[10] which indicates that pQCD fails badly at the ISR energies at high  $x_F$ . For the  $3^\circ$  data compared in that paper the calculation under predicts the data by up to an order of magnitude, but this is at larger  $x_F$  than we have data for here. The slight discrepancy seen near 1.5 GeV/c for  $y=3.1$ , may reflect the similar trend. We do conclude that in the  $p_T$ -range of 1-1.5 GeV/c the calculation reproduces the data for  $\pi^-$  within 20% thus making the use of perturbative description in the transverse spin asymmetries well justified as described in a forthcoming paper[18].

We have investigated the data of Owens[11] as given in the Durham HEP data repository further. The data are given for 4 angle settings in the forward region with mean angles of  $\Theta = 3, 57.5$  and  $10$  degrees. We observe that the  $p_T$  distribution in each setting has the same dependence for each setting, but stops at the kinematic limit. This kind of behaviour is not

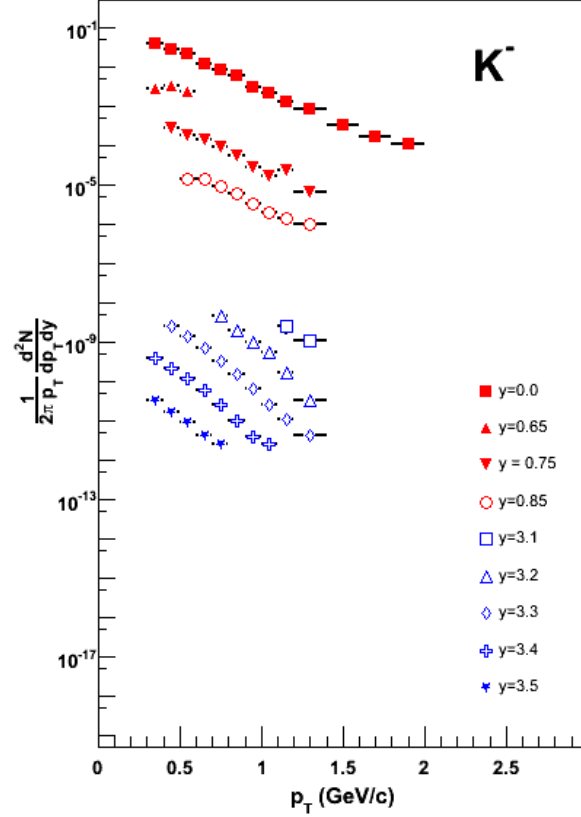


FIG. 9: Invariant rapidity densities for  $K^-$  for rapidities as indicated in the figure. Each rapidity bin is scaled down by a factor of 10 from the previous

expected since meson production is usual suppressed near the kinematic limit. This is e.g. seen in the data of [19] that for a fixed angle at 53 GeV show that the cross section start falling rapidly within 20% of the kinematic limit. We therefore are cautious to put to much weight on the data of [11]. It is thus possible that the data have problems e.g. because the  $\pi^0$  spectra are deduced from the inclusive photons spectrum, that the angular resolution of the detector is so large that the rapidly changing cross section with angle is not taken properly into account.

limited fragmentation. ??

comparison to OLD ISR data, identified

comparison to 'usual used pion spectrum at 62 GeV.. d''Enteria []

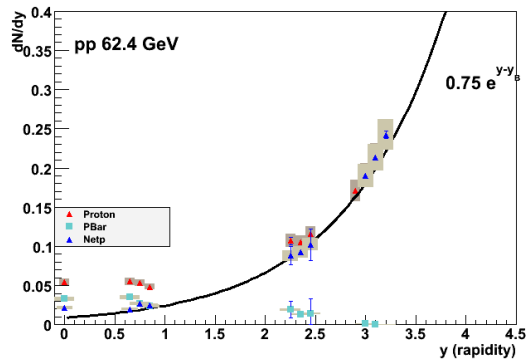


FIG. 10: Invariant rapidity densities for protons, anti-protons, and net protons. Net-protons are compared to the simple expectation assuming  $dn/dx$  being constant.

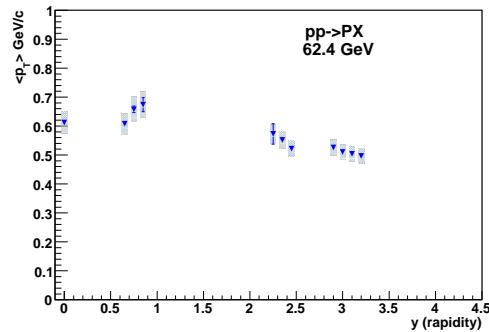


FIG. 11: Mean  $P_t$  vs. rapidity for Protons.

comparison to Pythia (version, tweak parameters?)

com

counting rules??

The pion spectra in  $p + p$  collisions, discussed in the introduction of this chapter can be

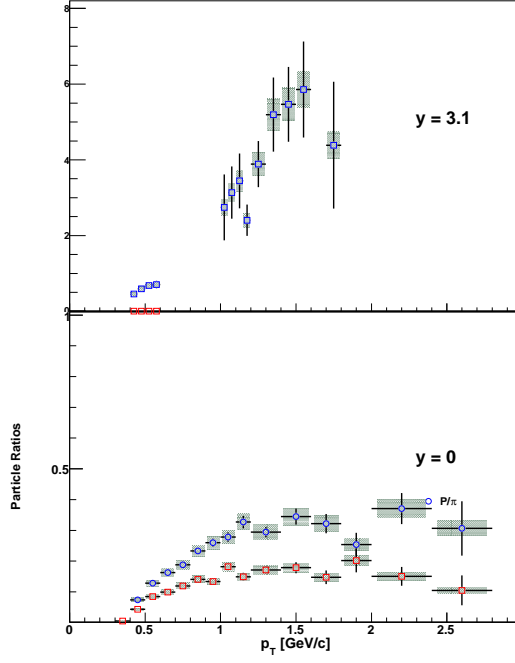


FIG. 12: Particle ratio of protons over pions for  $p/\pi^+$  and  $\bar{p}/\pi^-$  at mid-rapidity (lower panel) and high rapidity ( $y = 3.1$ ) top panel.

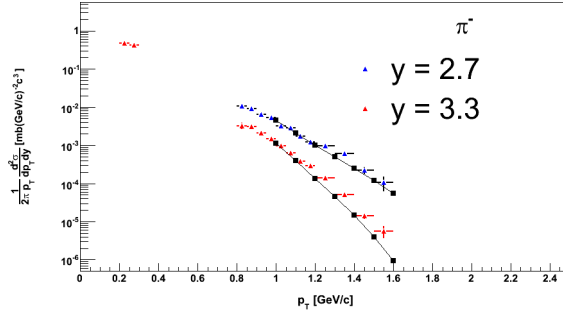


FIG. 13: Invariant transverse spectra for  $\pi^-$  at 2.7 and 3.3 compared with NLO pQCD calculations as described in the text. (prelim figure -placeholder)

compared to the empirical function in equation 7.3, proposed by D. d'Enterria in [5]. were fitted to an empirical function  $A(e^{ap_t+bp_t^2} + p_T/p_0)^{-n}$

Since many of the experiments had wide rapidity bins, and equation 7.3 was fitted to data from many different experiments, the average of the  $(\pi^+ + \pi^-)/2$  spectra at  $y = 0$ . The  $p_T$  spectrum can be seen in the left panel of Fig. The D. d'Enterria function is drawn together with the spectrum. The right panel shows this spectrum divided by the function.

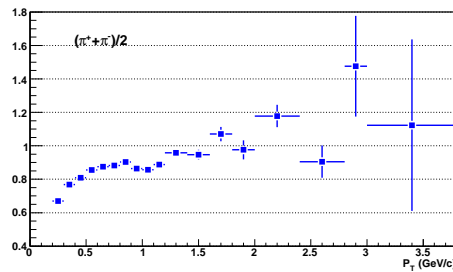


FIG. 14: Invariant transverse spectra  $(\pi^+ + \pi^-)/2$  at  $y=0$  divided by the global fit from Denterria.

The BRAHMS data are  $\approx 5\%$  lower than the parametrisation, but, apart from that, show agreement with parametrisation, within 10%.

### A. Other model comparisons

In addition to the pQCD comparisons models like PYTHIA[20] are often used to describe pp collisions. Most of the data in the rpresent paper are at relative low  $p_T$ so the strength of this model which is really at higher  $Q^2$  is not so obvious. Never the less we have compared several results of the present data with output from the default PYTHIA (version 6.319).

what to look at

i) dndy

ii) pi,K,p at  $y \sim 0$

iii) pi, p at high rap

iv) p/pi at low and high rap

comments on non choice of parameters i.e. no tune for these

## V. ACKNOWLEDGMENTS

We thank the staff of the Collider-Accelerator and Physics Departments at BNL for their vital contributions. We thank Werner Vogelsang for providing us with the NLO pQCD calculations shown in this paper. This work was supported by Brookhaven Science Associates, LLC under Contract No. DE-AC02-98CH10886 with the U.S. Department of Energy and by a sponsored research grant from Renaissance Technologies Corporation, the Danish Natural Science Research Council, the Research Council of Norway, The Polish State Committee for Scientific Research and the Romanian Ministry of research.

- 
- [1] I. Arsene *et al.*, BRAHMS, Nuclear Physics A **757**, 1 (2005).
  - [2] B. B. Back *et al.*, PHOBOS, Nuclear Physics A **757**, 28 (2005).
  - [3] J. Adams *et al.*, STAR, Nucl. Phys. **A757**, 102 (2005), nucl-ex/0501009.
  - [4] K. Adcox *et al.*, PHENIX, Nucl. Phys. **A757**, 184 (2005), nucl-ex/0410003.
  - [5] D. d’Enterria, J.Phys **G31**, S491 (2005).
  - [6] D.L.Adams *et al.*, E704 Collaboration, Phys. Lett. **B264**, 462 (1991).
  - [7] A.Bravar *et al.*, E704 Collaboration, Phys. Rev. Lett. **77**, 2626 (1996).
  - [8] BRAHMS Collaboration, *Single Spin Asymmetries of Identified Hadrons in Polarized  $p+p$  at  $\sqrt{s} = 62.4$  GeV and 200 GeV*, 2006.
  - [9] U. D’Alesio and F. Murgia, Phys. Rev. **D70**, 074009 (2004), hep-ph/0408092.
  - [10] C.Bourrely and J.Soffer, Eur.Phys.J **J36**, 371 (2004).
  - [11] Owen *et al.*, Phys. Rev. Lett. **45**, 89 (1980).
  - [12] R.Debbe *et al.*, BRAHMS Collaboration, Nucl. Instr. Meth. **A570**, 216 (2007).
  - [13] M.Adamczyk *et al.*, BRAHMS Collaboration, Nucl. Instr. Meth. **A499**, 437 (2003).
  - [14] I.Arsene *et al.*, BRAHMS Collaboration, Phys. Review C **A570**, 216 (2005).
  - [15] B.Budick and others (in preparation), Nucl. Instr. Meth. **1**, 1 (2007).
  - [16] *GEANT program library*.
  - [17] I.Arsene *et al.*, BRAHMS Collaboration, Phys. Review Letters **98**, 252001 (2007).
  - [18] I.Arsene *et al.*, BRAHMS Collaboration, Phys. Rev. Lett. (2007), arXiv:0801.1078.
  - [19] M. Albrow *et al.*, Nucl. Phys. **B56**, 333 (1973).

- [20] S. T. *et al.*, *Comp. Phys. Commun.* **135**, 238 (2001).
- [21] B. Jager, A. Schafer, M. Stratmann, and W. Vogelsang, *Physical Review D* **67**, 054005 (2003).
- [22] M. Banner *et al.*, *Nucl. Phys.* **B126**, 61 (1977).
- [23] A. Breakstone *et al.*, Ames-Bologna-CERN-Dortmund-Heidelberg-Warsaw, *Z. Phys.* **C69**, 55 (1995).
- [24] B. Alper *et al.*, British-Scandinavian ISR, *Phys. Lett.* **B44**, 521 (1973).
- [25] B. Alper *et al.*, British-Scandinavian ISR, *Phys. Lett.* **B44**, 527 (1973).
- [26] B. Alper *et al.*, *Phys. Lett.* **B47**, 275 (1973).
- [27] B. Alper *et al.*, *Phys. Lett.* **B47**, 75 (1973).
- [28] B. Alper *et al.*, British-Scandinavian, *Nucl. Phys.* **B100**, 237 (1975).
- [29] G. J. Alner *et al.*, UA5, *Z. Phys.* **C33**, 1 (1986).
- [30] M. Aguilar-Benitez *et al.*, *Z. Phys.* **C50**, 405 (1991).
- [31] C. Alt *et al.*, NA49, *Eur. Phys. J.* **C45**, 343 (2006), hep-ex/0510009.